Measurements of the CKM Angle β

Rainer Bartoldus

Stanford Linear Accelerator Center
2575 Sand Hill Rd
Menlo Park, CA 90025

Abstract. In this article I report on new and updated measurements of the *CP*-violating parameter β (ϕ_1), which is related to the phase of the Cabibbo-Kobayashi-Maskawa (CKM) quark-mixing matrix of the electroweak interaction. Over the past few years, β has become the most precisely known parameter of the CKM unitarity triangle that governs the *B* system. The results presented here were produced by the two *B* Factories, *BABAR* and Belle, based on their most recent datasets of over 600 million $B\bar{B}$ events combined. The new world average for $\sin 2\beta$, measured in the theoretically and experimentally cleanest charmonium modes, such as $B^0 \to J/\psi K_S^0$, is $\sin 2\beta = 0.685 \pm 0.032$. In addition to these tree-level dominated decays, independent measurements of $\sin 2\beta$ are obtained from gluonic $b \to s$ penguin decays, including $B^0 \to \phi K_S^0$, $B^0 \to \eta' K_S^0$ and others. There are hints, albeit somewhat weaker than earlier this year, that these measurements tend to come out low compared to the charmonium average, giving rise to the tantalizing possibility that New Physics amplitudes could be contributing to the corresponding loop diagrams. Clearly, more data from both experiments are needed to elucidate these intriguing differences.

Keywords: CP violation, CKM matrix, unitarity triangle, b->s gluonic penguins
PACS: 12.15.Hh, 13.25.Hw, 13.20.He

THE CKM MATRIX

Flavor transitions in the quark sector of the Standard Model are described by the Cabibbo-Kobayashi-Maskawa (CKM) matrix, which links the weak eigenstates of the three generations to their mass eigenstates. To maintain universality of the total coupling strength, the CKM matrix must be unitary. This leaves it with only four free parameters: three rotation angles and one complex phase. All other phases can be absorbed in the quark fields. In the Standard Model, *CP* violation is generated by this one irreducible phase of the CKM matrix.

The B Unitarity Triangle

The unitarity condition leads to six relations of the form $V_{ud}V_{ub}^* + V_{cd}V_{cb}^* + V_{td}V_{tb}^* = 0$, which are geometrically represented as triangles in the complex plane. They all have equal area, but only two of them have sides of the same order, and thus naturally large angles. Of these, the above unitarity relation is the one that controls *B* decays and $B_d\bar{B}_d$ mixing. The corresponding triangle is conveniently represented in the parameters $\overline{\rho}$ and $\overline{\eta}$ [1][2], which give the location of its apex (see figure 4). The angle at the far point on the real axis is $\beta = \arg(-\frac{V_{cd}V_{cb}^*}{V_{td}V_{tb}^*})$. A non-zero value of β implies *CP* violation.

$B\overline{B}$ Mixing

The second order weak interaction that causes the B and $\overline{B}$ flavor eigenstates to oscillate between each other is described by a pair of box diagrams involving W and top exchange. (Other quarks are CKM-suppressed.) As in the neutral kaon system, the B mass eigenstates are superpositions of the flavor eigenstates: $B_{\mathrm{H}} = p|B\rangle + q|\overline{B}\rangle$ and $B_{\mathrm{L}} = p|B\rangle - q|\overline{B}\rangle$. The oscillation frequency is given by the mass difference of the heavy and the light states, $\Delta m_d = m(B_{\mathrm{H}}) - m(B_{\mathrm{L}})$. The box diagrams involve the CKM element V_{td}, which can to good approximation be written as $V_{td} \approx |V_{td}|\mathrm{e}^{-i\beta}$. Thus, via mixing, the B meson picks up a weak phase of $\frac{q}{p} = \mathrm{e}^{-2i\beta}$.

TIME-DEPENDENT CP ASYMMETRIES

Coherent Production of $B\overline{B}$

It is worth recalling that in $\Upsilon(4S) \rightarrow B\overline{B}$ there is – at any time – exactly one B_{H} and one B_{L} (mass eigenstates), one B and one $\overline{B}$ (flavor eigenstates), as well as one $B_{CP=+1}$ and one $B_{CP=-1}$ (CP eigenstates). It is this coherency that enables one to use the flavor tagging techniques to see the interference between the two B mesons in the event.

Interference between Mixing and Decay

As CP eigenstates can be reached by the decay of both the B and the $\overline{B}$, there is interference between decays with and without mixing. For a final state $f_{\pm}$, where $\pm$ denotes the flavor of the decaying B to be B or $\overline{B}$, the decay rate as a function of the B proper time, Δt, can be written as

$$f_{\pm}(\Delta t) = \frac{1}{4\tau_B}\mathrm{e}^{\frac{-|\Delta t|}{\tau_B}}\left[1 \pm S_f \sin(\Delta m_d \Delta t) \mp C_f \cos(\Delta m_d \Delta t)\right].$$

Here, τ_B is the B^0 lifetime, and the coefficients S_f and C_f for the sine and cosine term are

$$S_f = \frac{2\,\mathrm{Im}\,\lambda}{1 + |\lambda|^2}, \qquad C_f = \frac{1 - |\lambda|^2}{1 + |\lambda|^2},$$

where

$$\lambda = \frac{q}{p}\frac{\overline{A}(\overline{B} \rightarrow f_{CP})}{A(B \rightarrow f_{CP})}$$

depends on the amplitude ratio of the $\overline{B}$ and the B decay. It is the (surprisingly) long B lifetime, which is comparable to the oscillation frequency, $(1/\tau_B \approx 0.5\,\mathrm{ps}^{-1}, \Delta m_d \approx 1.5\,\mathrm{ps}^{-1})$ that makes mixing observable. The sine term (S_f) arises from the interference between direct decay and decay after one net B-$\overline{B}$ oscillation. A non-zero cosine term (C_f) would arise from the interference between decay amplitudes with different weak and strong phases (direct CP violation) or from CP violation in $B\overline{B}$ mixing.

CP Asymmetry

Using this, one can compute the time-dependent *CP* asymmetry, which becomes

$$A_{CP}(t) \equiv \frac{\Gamma(\overline{B}(t) \to f_{CP}) - \Gamma(B(t) \to f_{CP})}{\Gamma(\overline{B}(t) \to f_{CP}) + \Gamma(B(t) \to f_{CP})} = S_f \sin(\Delta m_d \Delta t) - C_f \cos(\Delta m_d \Delta t).$$

Again, S_f is non-zero if there is *CP* violation in the interference between decays with and without mixing. A non-zero value for C_f implies direct *CP* violation. In the absence of additional amplitudes with different weak phases, and observing that in the Standard Model *CP* violation in mixing is negligible, one has $|\lambda| \approx 1$ and, to an excellent approximation, $S_f = \text{Im}\,\lambda$ and $C_f = 0$. Hence, in this situation, which is the case for the charmonium final states, and to some approximation for the $b \to s$ penguins, the sine coefficient becomes $S_f = \sin 2\beta$.

THE ASYMMETRIC *B* FACTORIES *BABAR* AND BELLE

The two *B* factory experiments, *BABAR* at SLAC in the US, and Belle at KEK in Japan, started operations practically at the same time in 1999. Both facilities have an asymmetric beam energy configuration, with 9.0 GeV (e^-) on 3.1 GeV (e^+) at PEP-II, and 8.5 GeV (e^-) on 3.5 GeV (e^+) at KEKB, which leads to an effective boost of the $\Upsilon(4S)$ system along the beam axis of $\beta\gamma = 0.56$ and $\beta\gamma = 0.43$, respectively. This opens the possibility to reconstruct decay time differences between the two *B* mesons in the event by measuring the displacements of their decay vertices along the beam line. The cross section for $b\bar{b}$ production at the $\Upsilon(4S)$ resonance is about 1 nb, leading to 1 million $B\overline{B}$ pairs per fb^{-1}. To date, both facilities have (far) exceeded their design luminosities, taking that amount of data in only 1-2 days. This has resulted in unprecedented datasets for *B* physics and much beyond.

B Reconstruction

The general strategy for the reconstruction of *B* events is to exploit the kinematics of the $e^+e^- \to \Upsilon(4S) \to B\overline{B}$ process, in which *B* mesons are produced nearly at rest in the $\Upsilon(4S)$ center-of-mass (cm) frame. Two virtually uncorrelated kinematic variables are used to select *B* candidates: the so-called beam-energy constrained mass, $m_{EC} \equiv \sqrt{(E_{\text{beam}}^{\text{cm}})^2 - (p_B^{\text{cm}})^2}$, and the energy difference, $\Delta E \equiv E_B^{\text{cm}} - E_{\text{beam}}^{\text{cm}}$, where $E_{\text{beam}}^{\text{cm}}$ is the beam energy in the $\Upsilon(4S)$ cm frame, and E_B^{cm} and p_B^{cm} are the cm energy and momentum of the *B* candidate, respectively. Various multivariate techniques were developed that distinguish $B\overline{B}$ events from ($e^+e^- \to q\bar{q}$, $q = u,d,s,c$) continuum as well as from potential QED backgrounds such as Bhabha events. Many methods take advantage of the fact that $B\overline{B}$ event shapes tend to be spherical, whereas continuum background is more jet-like.
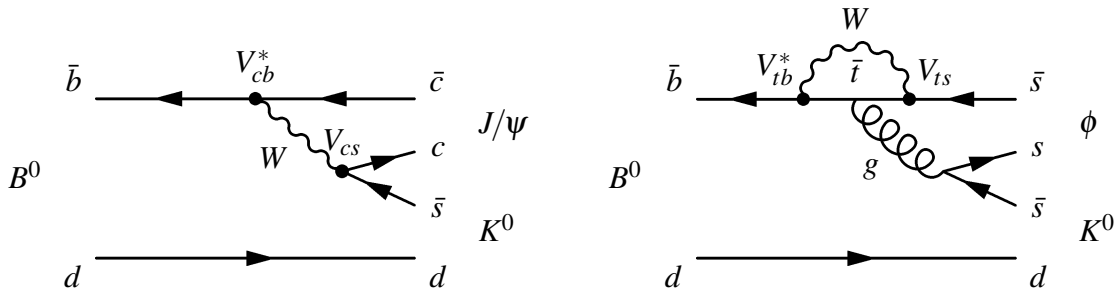
FIGURE 1. Feynman diagrams for *B* decays proceeding via tree (left) and penguin (right) transitions.

Time-Dependent CP Analysis

To extract the Δt distribution with high efficiency, both experiments have developed sophisticated flavor tagging techniques. One *B* meson is fully reconstructed in a *CP* eigenstate, which also determines its decay vertex. The other *B* is not reconstructed, but its flavor is determined ("tagged") to be either a *B* or a $\overline{B}$, from one of various tagging algorithms. These include, for example, lepton tags from semi-leptonic decays, kaon tags, soft pion tags from $D^*(2010)^\pm$ decays, etc. The tags are defined using multivariate algorithms, involving likelihood selectors or neural networks. A mistag probability, w, dilutes the observed asymmetry – and reduces the sine amplitude – by a factor $(1 - 2w)$. Thus, a figure of merit for the *CP* analysis is the effective tagging efficiency, $Q = \sum_i \varepsilon_i (1 - 2w_i)^2$, where ε_i is the tagging efficiency of mode *i*. Both experiments achieve an effective tagging efficiency that is very close to 30 %. The tagging vertex is determined from tracks not associated with the reconstructed *B* candidate. The measured separation between the two decay vertices, Δz, gives $\Delta t = \Delta z / \beta \gamma$. The time difference, Δt, is a signed quantity, as the principle applies whether the tagged *B* decays before or after the reconstructed *B*. The average separation $\langle \Delta z \rangle$ in the two experiments is about $100 - 200 \, \mu$m.

Trees and Penguins

The $b \rightarrow c\overline{c}s$ transitions are mediated by tree and penguin diagrams, with equal dominating weak phases. The $b \rightarrow s\overline{s}s$ transitions are pure penguin diagrams. Due to the high mass scales involved in the penguin loops, new particles could enter and contribute additional weak phases, thus giving rise to *CP* violation beyond the Standard Model. See figure 1 for the two main diagrams.
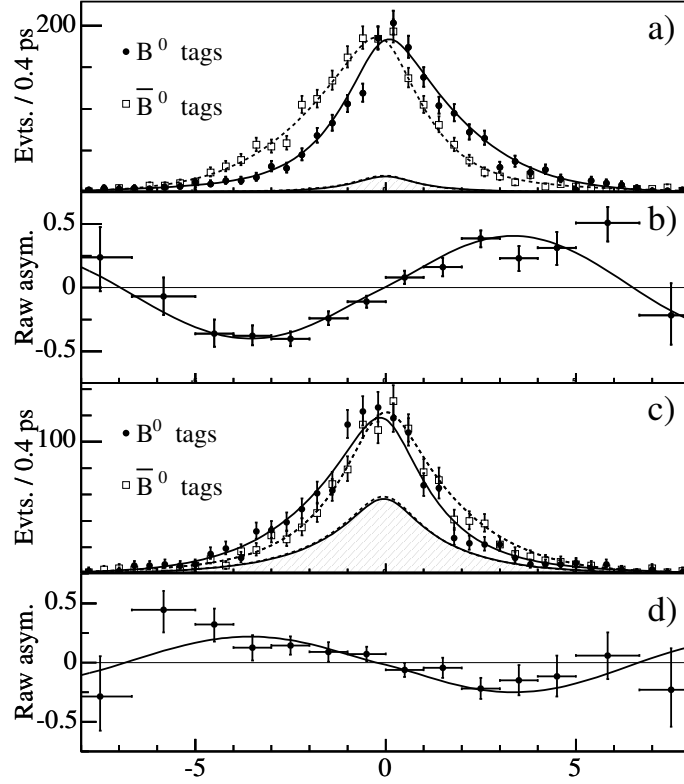
FIGURE 2. *BABAR* Δt distributions of candidates with B^0 and $\overline{B}^0$ tags for *CP*-odd (a) and *CP*-even (c) modes, and corresponding raw asymmetries (b and c). The solid curves represent the projection from the maximum likelihood fit.

SIN 2β FROM $B \to c\bar{c}K^0$ (CHARMONIUM)

The *CP* asymmetries in the proper-time distribution of neutral B decays into a charmonium and a K^0 meson provide a high-precision measurement of $\sin 2\beta$. In their analysis of $227 \times 10^6\, B\overline{B}$ decays *BABAR* exploits all currently accessible final states: $J/\psi K_S^0$, $J/\psi K_L^0$, $\psi(2S)K_S^0$, $\chi_c K_S^0$, $\eta_c K_S^0$ and $J/\psi K^{*0}(K^{*0} \to K_S^0\pi^0)$ [3]. Of these, the K_S^0 modes are *CP*-odd, the one including K_L^0 is *CP*-even, and the $J/\psi K^{*0}$ state involves contributions from either *CP* state, where the effective eigenvalue is computed from the relative fractions of odd and even orbital angular momenta. *BABAR* performs a global maximum likelihood fit with 65 free parameters, including – besides $\sin 2\beta$ – mistag fractions for all tagging categories, Δt resolution functions and time dependence for signal and background samples. From this, *BABAR* obtains

$$\sin 2\beta = 0.722 \pm 0.040 \pm 0.023, \qquad (BABAR)$$

where, as throughout this note, the first error is statistical and the second systematic. Figure 2 shows the Δt distributions and raw asymmetries.
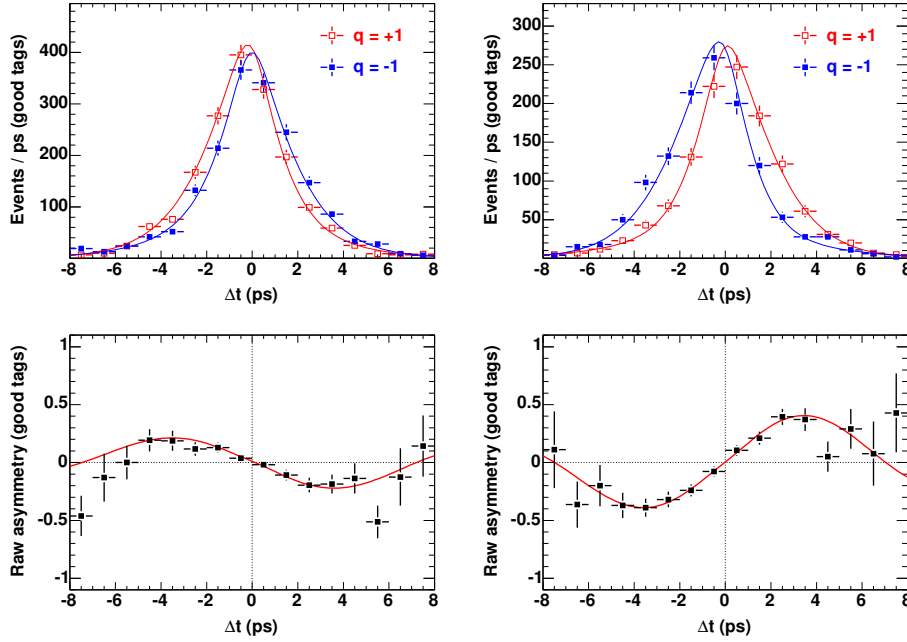
FIGURE 3. Belle Δt distributions (top) in $J/\psi K_S^0$ (left) and $J/\psi K_L^0$ (right) final states for B^0 and $\overline{B}^0$ tags, and corresponding raw asymmetries (bottom). The data shown corresponds to "good" ($0.5 < r \leq 1$) tags. The curves show the result of the maximum likelihood fit.

The very recent Belle analysis is based on $386 \times 10^6 B\overline{B}$ pairs, while focusing on the final states $J/\psi K_S^0$ and $J/\psi K_L^0$ [4]. Belle divides the data using an event-by-event flavor tagging dilution factor r, determined from Monte Carlo, that varies from 0 for no flavor discrimination to 1 for unambiguous flavor assignment. For the fit procedure, Belle takes a somewhat complementary approach to *BABAR*, where resolution functions and mistag fractions are determined in a first, separate multiparameter fit to various control samples, leaving only the two coefficients S_f and C_f as free parameters in the final maximum likelihood fit. The new Belle result is

$$\sin 2\beta = 0.652 \pm 0.039 \pm 0.020. \qquad \text{(Belle)}$$

The Δt distributions and raw asymmetries are shown in figure 3.

UT Constraints in the $\overline{\rho}$-$\overline{\eta}$ Plane

Combining the results from the two experiments with all available inputs is among the charges of the Heavy Flavor Averaging Group [5]. The result for $\sin 2\beta$ is to be compared with information from other measurements that provide constraints on the Unitarity Triangle. This information can be neatly presented as allowed regions of various shapes in the $\overline{\rho}$-$\overline{\eta}$ plane. Figure 4 shows the allowed regions from $\sin 2\beta$, from the other two UT angles, α and γ, from the measurement of $|V_{ub}/V_{cb}|$, as well as from the B_d^0 and B_s^0 mixing results for Δm_d and Δm_s, and from ε_K from *CP* violation in the *K* system.
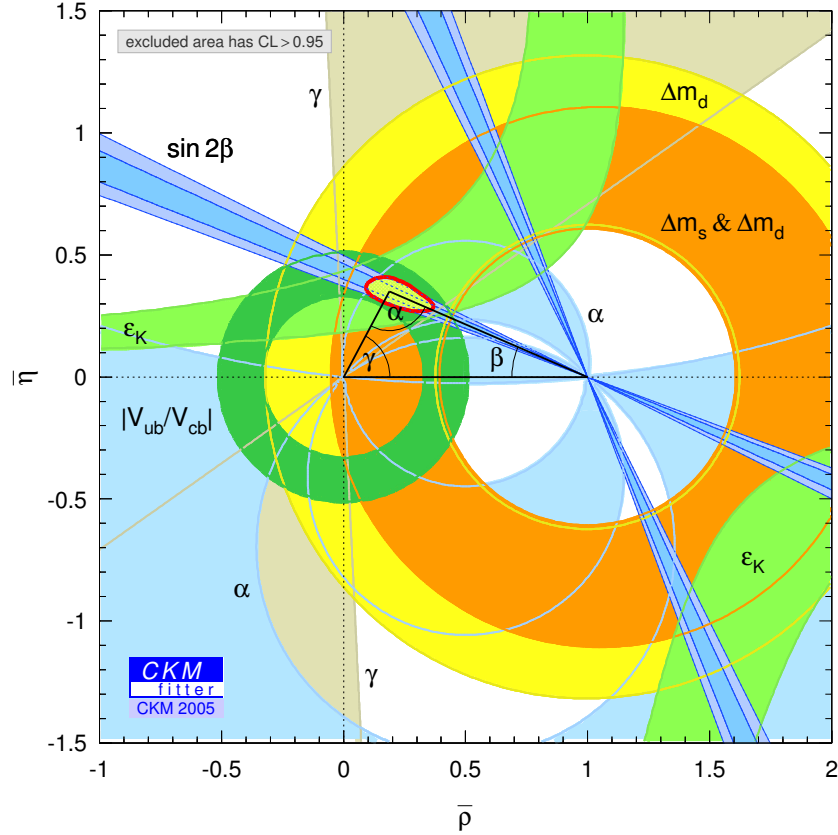
FIGURE 4. Constraints in the $(\overline{\rho}, \overline{\eta})$ plane using all available inputs, including the most recent β measurements, in the global CKM fit.

It can be seen that the $\sin 2\beta$ results are in remarkable agreement with all other UT measurements. This shows that the CKM mechanism is indeed the main source of *CP* violation. Combining these constraints in a global fit, as performed by the CKMfitter group [6, 7], leaves only a small allowed region for the position of the $(\overline{\rho}, \overline{\eta})$ apex.

UT Constraints from Angles alone

If one ignores the inputs from the UT sides, from *B* mixing and from the *K* system, one is left with only the angle measurements, *i.e.*, measurements of *CP* violation in the *B* system. A combined fit to only these inputs returns an allowed $\overline{\rho} - \overline{\eta}$ region very close to that of the full fit, demonstrating that today most of the constraint comes from the angles alone (figure 5). This can be seen as a milestone for the *B* Factories and illustrates how powerful they are. Moreover, $\sin 2\beta$ is the first UT input that is not limited by theory uncertainties.

It should also be noted that one can resolve the ambiguity in the sign of $\cos 2\beta$ by a time-dependent angular analysis of the vector-vector final state $J/\psi K_0^*(1430)$, which disfavors the solution with the larger $\sin 2\beta$ value at the 95 % confidence level [8][9].
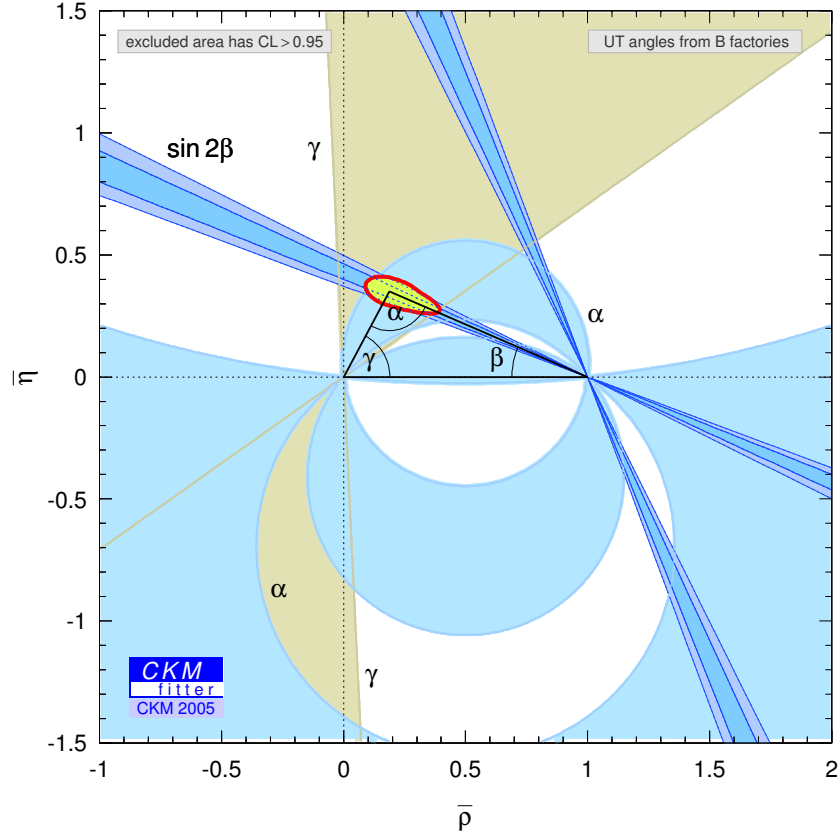
FIGURE 5. Constraints in the $(\overline{\rho}, \overline{\eta})$ plane including only the angle measurements in the CKM fit.

SIN 2β FROM $b \to q\overline{q}s$ PENGUINS

The effective $\sin 2\beta$ values, $\sin 2\beta_{\text{eff}}$, from the sine coefficient in penguin modes, are expected to agree with the charmonium values to within a few percent. Uncertainties are smallest for the pure penguin modes, $B^0 \to \phi K^0$ and $B^0 \to K_S^0 K_S^0 K_S^0$, and larger for the other modes, due to a possible $b \to u$ transition that carries a weak phase γ. Larger deviations would indicate a new *CP*-violating weak phase beyond the Standard Model. As already mentioned, large virtual mass scales are involved in the penguin loops, which may lead to additional diagrams with new heavy particles. A program is underway to measure as many of these modes as possible [10, 11, 12, 13, 14, 15, 16][4].

$B^0 \to \phi K^0$

The decay mode $B^0 \to \phi K^0$ is dominated by the gluonic penguin transition $b \to s\overline{s}s$. The neutral kaon is reconstructed in the *CP*-odd mode as K_S^0, from $K_S^0 \to \pi^+\pi^-$ and $K_S^0 \to \pi^0\pi^0$, and in the *CP*-even mode as K_L^0, using calorimeter and muon chamber signatures [10, 4].

$$B^0 \rightarrow K^+K^-K^0_S$$

The decays $B^0 \rightarrow K^+K^-K^0_S$, excluding the resonant ϕK^0_S contribution, are in general not CP eigenstates but rather an admixture of CP-even (f_+) and CP-odd (f_-) components. The CP eigenvalue depends on the angular momentum of the K^+K^- system: it is CP-odd for a relative P-wave, and CP-even for an S-wave. The observed sine coefficient therefore becomes $S_f = (2f_+ - 1)\sin 2\beta_{\text{eff}}$. To obtain $\sin 2\beta_{\text{eff}}$, the fraction f_+ needs to be determined experimentally. *BABAR* and Belle follow different approaches. *BABAR* performs an angular moment analysis based on the helicity angle distribution of one of the charged K mesons to extract the CP-even content as $f_+ = 0.89 \pm 0.08 \pm 0.06$ [10]. Belle also finds the state to be predominantly CP-even by using an isospin relation which yields $f_+ = 0.93 \pm 0.09 \pm 0.05$ [4].

$$B^0 \rightarrow \eta' K^0$$

The $B^0 \rightarrow \eta' K^0$ decay is another theoretically clean mode. It also enters with the highest branching fraction of all $b \rightarrow s$ penguin modes being investigated. The η' meson is reconstructed in the decays $\eta' \rightarrow \rho^0 \gamma$ and $\eta' \rightarrow \eta \pi^+ \pi^-$ with $\eta \rightarrow \gamma\gamma$ or $\eta \rightarrow \pi^+\pi^-\pi^0$. *BABAR* reconstructs the K^0_S, Belle also includes the K^0_L [11, 4].

$$B^0 \rightarrow \pi^0 K^0_S$$

The mode $B^0 \rightarrow \pi^0 K^0_S$ obviously poses a challenge for the reconstruction of the CP decay vertex. A method has been developed that exploits the knowledge of the average interaction point (IP), which is determined on a run-by-run basis from the spatial distribution of two-prong events. By constraining the single K^0_S trajectory to this IP, Δt is computed in a geometric fit. The sensitivity is further improved by constraining the sum of the two B decay times to $2\tau_B$ [13, 4].

$$B^0 \rightarrow K^0_S K^0_S K^0_S$$

With no charged track coming from the IP, the $B^0 \rightarrow K^0_S K^0_S K^0_S$ decay vertex has to be reconstructed using the same IP-constraint method pioneered for the mode $\pi^0 K^0_S$. At least two K^0_S are reconstructed in $K^0_S \rightarrow \pi^+\pi^-$, allowing one to be $K^0_S \rightarrow \pi^0\pi^0$. Theoretically, the $B^0 \rightarrow K^0_S K^0_S K^0_S$ mode is as clean as $B^0 \rightarrow \phi K^0$, since there is no u quark in the final state, and it is dominated by the $b \rightarrow s\bar{s}s$ penguin transition [16, 4].

TABLE 1. Signal yields for the time-dependent *CP* analysis selection of all tree and penguin *B* decay modes.

Mode	*CP*	branching fraction (10^{-5})	*BABAR* signal yield	Belle signal yield
$J/\psi K_S^0$	-1	85 ± 5	3404	5264 ± 73
$J/\psi K_L^0$	$+1$		2788	4792 ± 105
$\psi(2S)K_S^0$	-1	62 ± 7	485	
$\chi_c K_S^0$	-1	40 ± 12	194	
$\eta_c K_S^0$	-1	116 ± 26	287	
$J/\psi K^{*0}$	-1	131 ± 7	572	
ϕK_S^0	-1	$0.86^{+0.13}_{-0.11}$	114 ± 12	180 ± 16
ϕK_L^0	$+1$		98 ± 18	78 ± 13
$\eta' K_S^0$	-1	6.3 ± 0.7	804 ± 40	830 ± 35
$\eta' K_L^0$	$+1$			187 ± 18
$K_S^0 K_S^0 K_S^0$	$+1$	$0.42^{+0.18}_{-0.15}$	88 ± 10	105 ± 12
$\pi^0 K_S^0$	-1	1.2 ± 0.1	186 ± 18	106 ± 14
$f_0(975)K_S^0$	$+1$		152 ± 19	145 ± 16
ωK_S^0	-1	$0.55^{+0.12}_{-0.10}$	92 ± 13	68 ± 13
$K^+ K^- K_S^0$	$0.89 \pm 0.08 \pm 0.06$ $0.93 \pm 0.09 \pm 0.05$	2.5 ± 0.2	452 ± 28	536 ± 29

Summary

Table 1 summarizes the selected $\sin 2\beta$ modes with their *CP* values, branching fractions and the event yields obtained by the two experiments. Figure 6 summarizes the $\sin 2\beta$ results from the gluonic penguin modes, adding averages between *BABAR* and Belle, in comparison with the new charmonium world average.

CONCLUSIONS

In this article I briefly reviewed measurements of β (ϕ_1) that were obtained by the *B* factory experiments, *BABAR* and Belle, from the analysis of two different sources: the theoretically and experimentally "golden" *B* decay modes into charmonium final states, $b \to c\bar{c}s$, and a number of gluonic penguin modes involving the transition $b \to s\bar{s}s$. The charmonium modes, having provided first evidence of *CP* violation outside the neutral *K* system only a few years ago, have now reached a precision of better than 5 % from both experiments combined. The remarkable agreement of $\sin 2\beta$ with other Unitarity Triangle constraints establishes the CKM mechanism as the dominant source of *CP* violation. At the same time it makes it a firm reference for SM tests. Corresponding measurements of time-dependent *CP* violation in $b \to s$ penguins, on the other hand, seem to reveal consistently lower values for $\sin 2\beta$, thus leaving room for possible contributions of New Physics that could enter the loops. Increasingly sophisticated analyses of these rather challenging modes on one side, and better theoretical calculations on the other, have helped shape our knowledge surrounding this apparent difference. At this point we

sin(2β^eff)/sin(2φ₁^eff)

$\sin(2\beta^{\text{eff}})/\sin(2\phi_1^{\text{eff}})$

HFAG
HEP 2005
PRELIMINARY

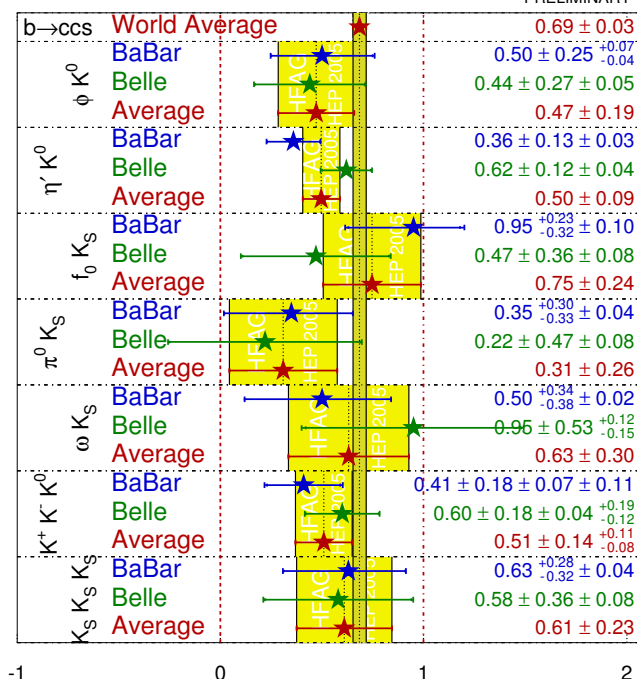|		
b→ccs	World Average	0.69 ± 0.03
φ K⁰	BaBar	$0.50 \pm 0.25\,^{+0.07}_{-0.04}$
	Belle	$0.44 \pm 0.27 \pm 0.05$
	Average	0.47 ± 0.19
η′ K⁰	BaBar	$0.36 \pm 0.13 \pm 0.03$
	Belle	$0.62 \pm 0.12 \pm 0.04$
	Average	0.50 ± 0.09
f₀ K_S	BaBar	$0.95\,^{+0.23}_{-0.32} \pm 0.10$
	Belle	$0.47 \pm 0.36 \pm 0.08$
	Average	0.75 ± 0.24
π⁰ K_S	BaBar	$0.35\,^{+0.30}_{-0.33} \pm 0.04$
	Belle	$0.22 \pm 0.47 \pm 0.08$
	Average	0.31 ± 0.26
ω K_S	BaBar	$0.50\,^{+0.34}_{-0.38} \pm 0.02$
	Belle	$0.95 \pm 0.53\,^{+0.12}_{-0.15}$
	Average	0.63 ± 0.30
K⁺ K⁻ K⁰	BaBar	$0.41 \pm 0.18 \pm 0.07 \pm 0.11$
	Belle	$0.60 \pm 0.18 \pm 0.04\,^{+0.19}_{-0.12}$
	Average	$0.51 \pm 0.14\,^{+0.11}_{-0.08}$
K_S K_S K_S	BaBar	$0.63\,^{+0.28}_{-0.32} \pm 0.04$
	Belle	$0.58 \pm 0.36 \pm 0.08$
	Average	0.61 ± 0.23

FIGURE 6. Compilation of results for $\sin 2\beta$ from charmonium and *s* penguin decays.

cannot know if the discrepancy is going to go away – as all others have in the history of the Standard Model – or whether it might indeed reveal the first hint of New Physics. We shall look forward to more results from the *B* factories, who in their continued operation each expect to quadruple the statistics of their datasets in the coming three years.

ACKNOWLEDGMENTS

REFERENCES

1. L. Wolfenstein, *Phys. Rev. Lett.* **51**, 1945 (1983).
2. A. J. Buras, M. E. Lautenbacher, and G. Ostermaier, *Phys. Rev.* **D50**, 3433–3446 (1994), `hep-ph/9403384`.
3. B. Aubert, et al., *Phys. Rev. Lett.* **94**, 161803 (2005), `hep-ex/0408127`.
4. K. Abe, et al. (2005), `hep-ex/0507037`.
5. HFAG, Unitarity triangle parameters (2005), URL `http://www.slac.stanford.edu/xorg/hfag/triangle/summer2005`.
6. J. Charles, et al., *Eur. Phys. J.* **C41**, 1–131 (2005), `hep-ph/0406184`.
7. J. Charles, et al., Results as of lepton-photon 2005 (2005), URL `http://www.slac.stanford.edu/xorg/ckmfitter/ckm_results_summer2005.html`.
8. B. Aubert, et al., *Phys. Rev.* **D71**, 032005 (2005), `hep-ex/0411016`.
9. R. Itoh, et al., *Phys. Rev. Lett.* **95**, 091601 (2005), `hep-ex/0504030`.
10. B. Aubert, et al., *Phys. Rev.* **D71**, 091102 (2005), `hep-ex/0502019`.
11. B. Aubert, et al. (2005), `hep-ex/0507087`.
12. B. Aubert, et al. (2004), `hep-ex/0408095`.
13. B. Aubert, et al., *Phys. Rev.* **D71** (005)), `hep-ex/0503011`.
14. B. Aubert, et al. (2005), `hep-ex/0503018`.
15. B. Aubert, et al. (2005), `hep-ex/0507016`.
16. B. Aubert, et al. (2005), `hep-ex/0507052`.